"ANALYSIS OF PARAMETERS AFFECTING CORROSION IN REINFORCED CONCRETE WITH USE OF ADDITIVES"

A PROJECT REPORT

Submitted in partial fulfillment of the requirements for the award of the Degree of

BACHELOR OF TECHNOLOGY

IN

CIVIL ENGINEERING

Under the supervision of

Dr. Saurav

(Assistant Professor)

By

Hritick Shama (141650)

Vaibhav Mehta (141652)

to

JAYPEE UNIVERSITY OF INFORMATION TECHNOLOGY

WAKNAGHAT, SOLAN – 173 234

HIMACHAL PRADESH, INDIA

May, 2018

CERTIFICATE

This is to certify that the work which is being presented in the project title **"Analysis of Parameters Affecting Corrosion in Reinforced Concrete with use of Additives"** in partial fulfillment of the requirements for the award of the degree of Bachelor of technology and submitted in Civil Engineering Department, Jaypee University of Information Technology, Waknaghat is an authentic record of work carried out by **Hritick Shama (141650) and Vaibhav Mehta (141652)** during a period from July, 2017 to May, 2018 under the supervision of **Dr. Saurav** (Assistant Professor), Department of Civil Engineering, Jaypee University of Information Technology, Waknaghat.

The above statement made is correct to the best of my knowledge.

Date: - ....-May-2018

Dr. Ashok Kumar Gupta   Dr. Saurav   External Examiner

Professor & Head of Department   (Assistant Professor)

Department of Civil Engineering   Department of Civil Engineering

JUIT, Waknaghat   JUIT, Waknaghat

ACKNOWLEDGEMENT

Hritick Shama (141650)

Vaibhav Mehta (141652)

ABSTRACT

In this study, experimental investigation of Corrosion behavior in beams with respect to change in various parameters like W/C ratio, cover depth and reinforcement diameter is done. Corrosion in the beams were induced by impressed current technique. The Half-cell Potential method was used to calculate the probability of corrosion in the beams. The various trends and patterns were observed and highlighted. Strength characteristics of the specimens were also studied by calculating Flexural strength of beams using Center point loading method, both before and after Corrosion. The loss in the mass of the reinforcement was also calculated by faraday's law as well as from experimental data. Two additives were also added in combination. First is Alccofine-1203 which is ultrafine slag, used as 20% replacement of cement. It reduces the permeability of concrete, because of its fineness and packing efficiency, making it less resistant to corrosion. Other is Crimped Steel fibers 1% by weight of concrete. Main reason for adding steel fibers was to reduce the availability of oxygen and water to the reinforcement, hence hindering the electrochemical reaction at reinforcement. These additives were used separately as well as together to observe their effects.

<u>CONTENTS</u>

LIST OF FIGURES

LIST OF TABLE

LIST OF SYMBOLS

x

m = mass of steel consumed

I = current (A)

t = time (s)

F = 96,500 A.s

z = ionic charge (2 for Fe $\rightarrow$ Fe^{2+} + 2e^{-})

M = molar mass of metal (56g for Fe)

I_{corr} = corrosion current density (A)

E_{corr} = Corrosion Potential (V)

B = Empirical constant

R_p = Polarization resistance

ΔI = Change in current flow

ΔE = Change in Potential

w/c = Water-Cement ratio

F_{bt} = Modulus of rupture or flexural strength

P: Max total load

l: Span length between supports

d: depth of the beam

b: width of the beam

CHAPTER 1

INTRODUCTION

1.1   GENERAL

Reinforcement corrosion is one of the main causes of premature deterioration of reinforced concrete structures. The corrosion of reinforcement is one of the main causes of reduction in service life of reinforced concrete structures. The physical signs of corrosion like rust stains, spalling and cracking appear after the corrosion process has been significantly spread. The goal of this study is to estimate the extent to which the corrosion has spread according to half-cell potential values and its effect on the flexural strength of the reinforced concrete beams. The change in the half-cell potential values and the flexural strengths of corroded beams with the use of additives like crimped Steel Fibers and Alcofine-1203 were observed. Information about the corrosion behavior of the corroded beams will help in suggesting early warning of future durability problems and helps in recommending the appropriate remediation options to the owner of structure.

1.2   MECHANISM OF CORROSION

In the corrosion process, iron is oxidized to form iron oxides. The measure of the steel converted to oxides can be calculated directly from the electric potential values generated in the half-cell which undergoes anodic reaction as in Figure 1.1:

$$Fe \rightarrow Fe^{2+} + 2e^-$$

And consumed by the cathodic reaction:

$$H_2O + \tfrac{1}{2} O_2 + 2e^- \rightarrow 2OH^-$$
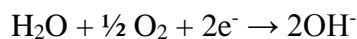
Metal loss can be calculated from Faraday's law:

$$m = \frac{MIt}{zF}$$
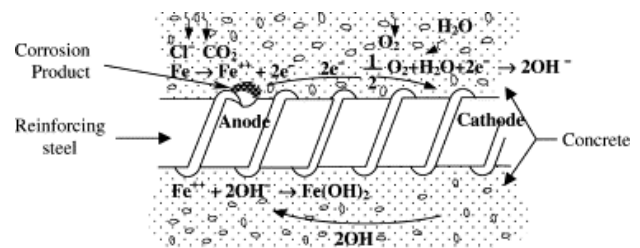
Figure 1.1 - Corrosion - Electrochemical Process [4]

1.3 HARMFUL EFFECTS OF CORROSION

Definitely there are many harmful effects of corrosion. Some of them are listed below.

i. Loss of Strength

Corrosion leads to the deterioration of the rebar and hence reduces its effective cross section. This reduces the flexural, the axial strength of reinforced beam and makes the structure poor. The corroded segments looks stable yet it doesn't mean that they are totally safe, in fact, due to the corrosion process the ultimate load that the structure can take reduces and it can even get lower than the design load of the structure and hence, making the structure unsafe. Both steel as well as reinforced concrete structures can be affected by Loss of strength. Corrosion under insulation (CUI) is a frequently observed in refineries, gas and oil industries. Steel sections which are covered under fireproofing insulation experience corrosion over their entire service life. The shear and flexural capacity of the RC element undergoing corrosion is also reduced.

ii. Fatigue

Corrosion has another structural effect i.e. on the fatigue strength of RC elements, steel elements, and connections. Corrosion can rapidly increase the propagation of fatigue crack in structural steels. Pitting corrosion leads to the introduction of stress concentrations at additional points at which cracking can be developed, hence the fatigue strength of concrete will be lowered.

iii. Reduced Bond Strength

The Load capacity depends on the characteristics of the concrete-rebar interface in composite elements such as RC sections. The volume of the byproducts of corrosion process is greater than the steel. This process generates a poor quality steel layer between the interface of the surface of concrete and the reinforcement surface. The layer formed has a poor interface with surrounding concrete, therefore, the capacity of the element is reduced. In case of lap splices or anchorage, this could decrease the effective length of anchorage, and leading to premature failure of sections.

iv. Limited Ductility

The ductility of corroded reinforced concrete beams starts reducing after the corrosion process starts. This is critical in earthquake load design and its evaluation. The plastic deformation of Corroded sections is limited because of significantly lower ductility after corrosion process. This affects the response of the elements to any earthquake load. The development of yield stress is prevented because the load transfer in the laps will be affected by Corrosion of reinforcement in the lap splices.

v. Reduced shear capacity

As the corrosion process undergoes the effective cross sectional area of reinforcement in beams and columns is reduced which reduces the shear capacity of the section. Chances of punching shear failure are increased in concrete slabs because the corrosion process reduces the shear strength of the slab near to the columns. The corrosion process can result in shear failure of the footings, flexural yielding, or anchorage failure of steel reinforcement in the footing.

1.4 FACTORS AFFECTING CORROSION

The corrosion of reinforcement is dependent on various factors some of which can be controlled to minimize corrosion and special measures can be taken for others. The following factors are responsible for corrosion of steel reinforcement in reinforced concrete structure.

i. Quality of concrete

The right quality of materials, i.e. cement, fine aggregate, coarse aggregate and water, with proper water to cement ratio, adequate mixing, correct compaction either by vibration or tamping and proper curing results in desired quality of concrete. There is perpetually an opportunity of corrosion of reinforcement when any of the above mentioned steps don't seem to be followed within the specific manner, leading to lesser quality of concrete. Dense concrete, i.e. High strength concrete is generally impervious to corrosion to large extent and protects the reinforcement steel.

ii. Cover thickness of concrete reinforcement

Concrete cover is like a protective layer over the reinforced steel which protects it from corrosion. The degree of protection against the various environmental and other climatic conditions is more when higher cover depth is provided. The cover depth for various structural members should show a discrepancy depending upon their importance and degree of exposure. For the protection of steel reinforcement against corrosion, correct evenness of concrete cover over the reinforcement steel is additionally necessary.

iii. Condition of reinforcement

The corrosion rate is also affected by the surface condition of the steel reinforcement at the time of its placing in concrete. The contamination of the reinforcement with salt or existing corrosion activity can promote the corrosive action on reinforcement after placement in concrete rapidly.

iv. Porosity of concrete

The penetration of the above mentioned chemicals is possible only due to permeability or porosity of the concrete. The porosity of concrete is dependent upon the size, distribution and continuity of capillary pores inside the concrete. This in turn is dependent upon the w/c ratio for given degree of hydration. The porosity also depends upon other factors, such as

- Type of cement
- The size and grading of aggregate
- Degree of compactness
- Age of concrete

v. Effect of environmental and other chemicals

Chemical originating from the environment or from within the concrete materials are the main source of deterioration process in RC sections. The first sign of deterioration of reinforced concrete is the development of cracks which are due to the attacks of these chemicals. The main chemical attacks which effects the corrosion process are due to the presence of carbonation, salt, chloride attack and reaction of sulphates with tricalcium aluminate (C_3A) present in cement.

Concrete is a mixture of aggregate, cement and water mixed intimately which is highly alkaline is its green state. Calcium hydroxide is developed during the hydration of cement which increases the pH value of the mix up to 12.5. The reinforcing steel, in such basic

conditions, is roofed with a film of oxides that protects the steel from the corrosion.

vi. Freezing and thawing condition

The water present as moisture in the pores of concrete freezes in the cod regions. The conversion of water to ice gives rise to volumetric expansion which may exceed the bursting pressure of surrounding concrete mass. This leads to increased corrosion action on reinforcement because of development of cracks in concrete.

vii. Effect of high thermal stress

A temperature up to 1000°C can be endured by any normal concrete. When the concrete is exposed to higher temperature then these the deterioration of concrete starts. In industrial plants and power stations, special protective measures are required in concrete otherwise the concrete may develop thermal cracks. Concrete structures are consequently a lot of affect by the environmental chemical after the crack formation and therefore the method of corrosion starts.

1.5 ELECTROCHEMICAL TECHNIQUES USED FOR DETERMINATION OF CORROSION

1.5.1 Half-Cell Potential Technique

The half-cell potential technique is the most commonly used technique of corrosion measurement of the steel rebar's for concrete. Such technique depends upon measurement from electrochemical potential of steel rebar among indication toward a usual reference electrode located upon the concrete's surface as well as might provide a indication of possibility of steel's corrosion. To improve contact among the concrete's surface as well as reference electrode a porous otherwise spongy plug is used. As a result of ASTM copper and copper sulfate electrode is a recommended reference electrode. Suggested guiding principles for analysis of half-cell potential outcomes agreeing to ASTM are listed in Table 3.1. It should be noticed that this technique does not find out real corrosion rate as well as corrosion's probability [7].

1.5.2 Electrochemical Impedance Spectroscopy

In recent years reputation of Electrochemical Impedance Spectroscopy (EIS) for toughened concrete has improved amazingly. Important facts regarding structure, double-layer capacitance, fresh reactions, corrosion rate, electrolyte environment resistance as well as interface can be supplied by investigation of system reaction. Electrochemical Impedance Spectroscopy examines the system reaction from system's impedance to the application of a little amplitude alternating potential generally 20 mV signal at dissimilar frequencies [7].

1.5.3 Linear Polarization Resistance

In the Linear Polarization Resistance (LPR) method, a fixed potential signal is employed for a definite time period, which is found out through the time for the current to attain stable situation in the shape of a square wave among the functioning electrode steel reinforcement in concrete as well as the reference electrode along with the reaction current I is calculated in LPR method. Corrosion current can be estimated by applying Stern–Geary equation and R_p [26].

1.5.4 Galvanodynamic Polarization

Galvanodynamic polarization is a technique in which continuously varying current at a selected rate is applied to an electrode rebar present in an electrolyte concrete pore solution. This method plots the change in potential versus the controlled current. This is a relatively fast method as compared to other methods to obtain the value of Rp, as well as the corrosion rate [7].

1.5.5 Potentiodynamic Cyclic Polarization

Potentiodynamic Cyclic Polarization is a cyclic Potentiodynamic polarization method which is comparatively non-damaging measurement that can grant data regarding the potential of corrosion, rate of corrosion as well as vulnerability toward metal pitting corrosion. This method is built upon the thought that forecasting's of the nature of a metal in an atmosphere can be prepared by pushing the matter from its stable state circumstance as well as supervising how it reacts to the push as the push is detached at a steady rate and the scheme is upturned to its stable state circumstance [7].

1.5.6 Gravimetry

To examine and establish the most suitable electrochemical corrosion measurement technique, all of beams were autopsied and each element was weighed and the amount of mass lost was determined. To execute the test, the corrosion products were removed using the Clark solution 1000 ml HCl with specific gravity = 1.19 + 20 g antimony trioxide Sb_2O_3 + 50 g stannous chloride $SnCl_2$. The test has been executed according to the ASTM G1-90 standard procedure. This prepared solution is efficient in cleaning the corrosion products at room temperature conditions. The steel elements were immersed in standard Clark solution until the corrosion products were completely vanished. The extent of the corroded area decides the time and could be more or less than 30 minutes. Due to the toxic or harmful nature of the Clark solution, the cleaning procedure must be executed under a fume hood with all safety measures. Using the area under the corrosion current density versus time curves, the effective mass loss was calculated and then compared with the real mass loss obtained with the help Gravimetry method [7].

1.6 MATERIALS

- Cement (PPC)
- Sand
- Aggregates (Angular)
- Steel Reinforcement (12mm, 16mm, 20mm) of grade Fe500
- Curing tank
- NaCl solution
- Steel fibers (crimped)
- Alccofine 1203
  Electrical Equipment
  - Power supply (mV)
  - Multimeter
  - Connection Wires

1.7 BENEFITS

- Increased structural life of concrete, particularly where chloride contamination is more likely.

- Adequate concrete cover over the steel reinforcement.

- Diminished effect of variations in concrete quality with time.

- Reduced likelihood of surface staining.

- Spalling of concrete will be delayed.

CHAPTER 2

LITERATURE REVIEW

2.1 GENERAL

All the experimental work done in this project was planned after constant literature review throughout the time period of the project. Many pieces of literature were thoroughly studied, few of them being extremely helpful in the experimental planning are mentioned below, and many others who provided crucial information both in planning and execution of experimental work.

Sravana Babu Parvatareddy and G. Ganesh Naidu, (2017), "Comparative Study on Various Methods Used for Corrosion Protection of Rebar in Concrete" [1] **-** In this paper, the five commonly used methods of protection of rebar against corrosion in concrete, which are; high grade concrete, use of inhibitors in concrete, concrete surface coating, rebar coating and cathodic protection, are experimentally compared. Bond strength is determined by carrying out pullout test at the end of corrosive exposure on all specimens. Mass loss in the rebar is determined for all rebar's after the pullout test. The relative advantages and disadvantages of all methods have been studied by comparing all these parameters with the control specimen which is unprotected.

S. Nabeel and S. Sheetal (2016), "Effect of impressed current on corrosion of reinforcing bar in reinforced concrete" [4] - In this experiment, three different voltages 4V, 6V and 10V were used and was impressed on reinforced bar in concrete. This work was carried out to study the effect of impressed current on corrosion rate of steel reinforcing bar in concrete. The study evaluated the time vs. crack, concrete crack pattern, and the mass loss due to accelerated corrosion up to the development of first visible crack on the surface of concrete specimen. It was concluded that as the bar diameter increases, mass loss also increases for every voltage applied and mass loss increases as the voltage decreases for any given diameter of reinforcement.

K. Venkateswara Rao et al, (2016), "An Experimental Study on Flexural Strength and Corrosion Properties of Reinforced Concrete Beams" [3] **-** This study was carried out on corroded and un-corroded reinforced concrete beams to investigate and compare their flexural strength and theoretically estimated steel loss after corrosion. The beams were corroded experimentally by accelerated corrosion technique using 5% NaCl and impressed current applied over a period of time. The corroded beams have flexural strength values less than the un-corroded beams. From the flexural strength and theoretically estimated steel loss values it was concluded that flexural strength mainly dependent upon the grade of the concrete whereas the estimated steel loss depends on the replacement of cement with fly ash. There is a little change in the flexural strength and considerable reduction in the steel loss when the percentage of fly ash is increased.

V. Kumar et al, (2013), "A study on corrosion of reinforcement in concrete and effect of inhibitor on service life of RCC" [5] **-** The study explains that 'permeability' which is a function of w/c ratio, affects the corrosion of rebar, w/c ratio control strength, durability and permeability of concrete and does not control the rate of corrosion. With an increase in the w/c ratio, in the study, it is observed that the depth of penetration of particular chloride threshold value increases and the permeability of hardened cement paste is increased 100 fold by increasing the w/c ratio from 0.35 to 0.45. Under accelerated corrosion Technique, the time of initiation of reinforcement corrosion in a sample with a w/c ratio of 0.4 is 2.15 to 1.77 times more as compared to a sample with a w/c ratio of 0.55. Once the corrosion process has started the rate of corrosion is independent of the cover thickness.

A. Poursaee, (2011), "Corrosion Measurement Techniques in Steel Reinforced Concrete" [7] - The different corrosion measurement techniques were studied and evaluated in order to determine the most precise method for determining the corrosion rate of steel bars in reinforced steel concrete. Reinforced concrete specimens were exposed to salt solution after casting and the corrosion activity of the bars was studied by half-cell potential, galvanostatic pulse polarization, Electrochemical Impedance Spectroscopy, potentiostatic linear polarization resistance, galvanodynamic polarization, and Potentiodynamic cyclic polarization. The results obtained by the methods mentioned above were then compared with

the actual mass loss of the steel bars due to corrosion and it shows that methods and techniques based on applying current are not as much reliable measuring techniques when compared to those based on applying potential.

Dimitri V. Val et al, (2009), "Experimental and Numerical Investigation of Corrosion-Induced Cover Cracking in Reinforced Concrete Structures" [8] - In the paper experimental and numerical investigation of corrosion-induced crack initiation and propagation was done. The paper also showed that the thicker the concrete cover the longer it will take to fully fill a crack because corrosion products do not fully fill corrosion-induced cracks in concrete immediately after the crack initiation as the cracks are gradually being filled over time.

Veerachai Leelalerkiet et al, (2004), "Analysis of half-cell potential measurement for corrosion of reinforced concrete" [9] - The corrosion of reinforcing steel-bars in the concrete slabs under cyclic wet and dry conditions was estimated applying only non-destructive evaluation techniques like the half-cell potential measurement. The three-dimensional boundary element method (BEM) was applied to study the current flows and potential distributions of reinforcement. The inverse boundary element method (IBEM) was then applied to get experimental results to identify the corrosion states. The investigation of the influence of a void on the potential distribution and current flow was also carried out. Results showed that the half-cell potential measurements were marginally more successful as compared with analytical results of current flow and potential distribution by BEM. It was explained that results by IBEM analysis identifies clearly the corroded areas.

Shamsad Ahmad, (2003), "Reinforcement corrosion in concrete structures, its monitoring and service life prediction—A review" [10]– In this paper, a review is presented on the methods utilized to monitor the rebar corrosion, methodologies that are utilized for the prediction of remaining service life of structures and mechanism of reinforcement corrosion. The assessment of the extent and causes of corrosion in reinforcement was done by using various electrochemical techniques. Empirical models and experimental methods were used for the prediction of the remaining service life of a corroding RC structure. Three measurement parameters, namely half-cell potential, concrete

resistivity and corrosion current density were used to obtain the information about the state of reinforcement corrosion.

2.2 RESEARCH GAPS

- Dependency of extent of corrosion and corrosion rate on various factors.
- Effect of corrosion on ductility of reinforcing bars.
- Convenient method of repairing corroded steel bar.
- Effect of bond loss of tension reinforcement on the flexural behavior of reinforced concrete beams
- Structural performance of corroded rebar's.
- Factors controlling cracking of concrete affected by reinforcement corrosion.

2.3 RESEARCH OBJECTIVES

- Study of corrosion rate with change in rebar diameter.
- Optimization of cover depth and W/C ratio to minimize corrosion.
- Study in Flexural strength of concrete after corrosion.
- Effects of Additives on Corrosion of reinforced concrete.

CHAPTER 3

METHODOLOGY

3.1 GENERAL

A corroding metal in an environment will be characterized by the corrosion potential, E_{corr}. This can be measured relative to a reference electrode (half-cell) using a voltmeter. The metal potential may be shifted ΔE by an external perturbation (e.g. an externally applied current, ΔI). This process is termed polarization. The polarization resistance (R_p) may be defined as the steady state resistance that the metal interface presents to a change in potential, ΔE when the perturbation ΔI is small. Typically ΔI is selected so that ΔE is no more than ± 20 mV. Values of 5 to 10 mV are commonly used.

3.2 EXPERIMENTAL TECHNIQUE AND SETUP

3.2.1   Half-Cell Method

Corroding and passive rebar's in concrete show a difference in electrical potential. A macro cell is generated and current flows between these areas. This electric field can be measured by suitable reference electrode (half-cell) placed on concrete surface as shown in Figure 5.1. The most negative values corresponds to corroding zones as discussed in Table 3.1 [9].

Table 3.1 - Probability of corrosion according to half-cell potential reading [9]

Measured potential (mV vs. CSE)	Corrosion probability
-200 mV $<$ E	90% no corrosion
-350 mV $\leq$ E $\leq$ -200 mV	Intermediate
E $\leq$ -350 mV	90% corrosion
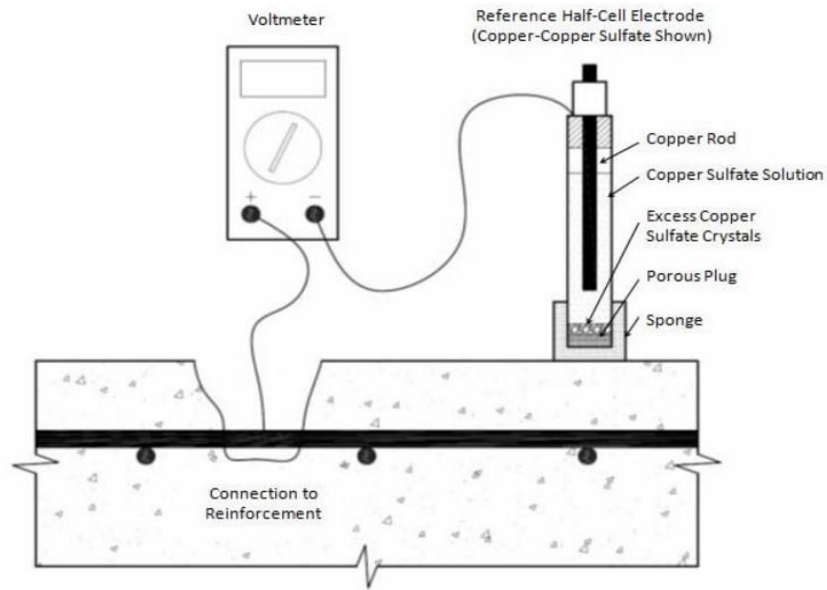
Figure 3.1 - Half Cell Method Setup

3.2.2 Flexural strength

Flexural Strength Using Center-Point Loading as shown in Figure 3.2 Modulus of rupture (F_{bt}) is given by:

$$F_{bt} = \frac{3Pa}{bd^2}$$

P: Max total load

a: length between line of fracture and the nearer support

d: depth of the beam

b: width of the beam

Figure 3.2 - Center point loading for calculation of Flexural strength

In RCC beams the main contribution to the flexural strength of beam is done by the reinforcement. The phenomenon of corrosion mainly attacks on the reinforcement, weakening it and hence decreasing the flexural strength of the whole beam. So, it is very important to study the flexural strength of beam undergoing the process of corrosion.

CHAPTER 4

EXPERIMENTAL ANALYSIS

The various test were performed on the materials to know their properties and create accurate mix design of M20 grade. The specimens were created according to the experimental data needed for the investigation

4.1 CEMENT

4.1.1 Normal Consistency (IS:4031-Part 4-1988)

The Consistency of cement test is performed to determine the amount of water percentage by weight of cement that is to be added in cement to attain Standard consistency or normal consistency of cement. It is the amount of water which when added to cement attains a penetration of 5-7 mm from the bottom of the Vicat's mould or 33-35mm from top of the Vicat's Mould as shown in Figure 4.1. Vicat's apparatus as per IS: 5513 was used [19].

The Normal Consistency of cement came out to be 34%.

Figure 4.1 - Vicat's apparatus

4.1.2 Initial setting time (IS:4031-part 5-1988)

The time at which cement starts hardens and completely loses its plasticity is called Initial setting time of cement. Within this time cement can be moulded in any desired shape without losing its strength. It is that time period between the time when water is added to cement and the time at which 1 mm square cross section needle Figure 4.2 fails to penetrate the cement paste, placed in the Vicat's

Figure 4.2 - Needle used for finding initial setting time of cement

mould (as per IS:5513) 5 mm to 7 mm from the bottom of the mould [20,19]. After doing the test initial setting time of cement is 40 minutes

4.1.3 Final setting time (IS:4031-part 5-1988)

The time at which cement completely loses its plasticity and became hard is a final setting time of cement. Final setting time is that time period between the time when water is added to cement and the time at which 5 mm attachment does not make any impression but 1 mm needle as shown in Figure 4.3 makes an impression on the paste in the mould of Vicat's apparatus [20].

Figure 4.3 - Needle with angular attachment used in Final setting time of cement

The cement paste in the mould of Vicat's apparatus was checked for final set after every hour. Final setting time of cement was determined to be 8 hours.

4.1.4 Specific gravity

Specific Gravity of Cement is the ratio of density of cement to density of water provided temperature remains constant. Excessive exposure of cement to moisture effects Workability and strength of cement. For Nominal mix design, the specific gravity of cement should be 3.15g/cc. If the cement is exposed to extreme moisture content due to bad weather conditions, then the specific gravity of cement may go up to 3.19. If the specific gravity is 3.19, then the pores in cement are filled with the moisture content. Cement undergoes Premature Hydration.
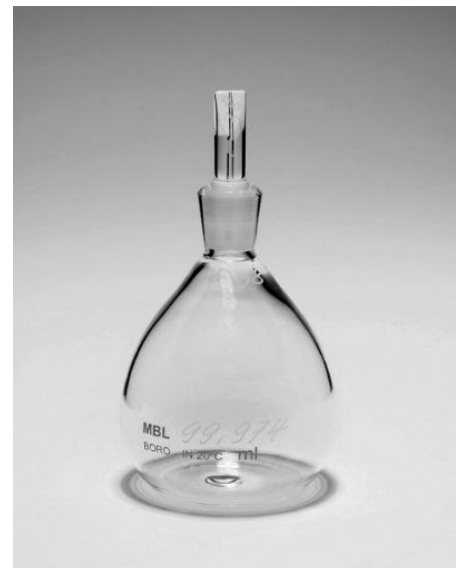
Figure 4.4 - Density bottle for determination of specific gravity

16

Specific gravity of cement is determined by density bottle method as in Figure 4.4. To calculate the specific gravity of material, we generally use water. But in cement, we use kerosene for finding specific gravity. Cement hydrates in the presence of water. Cement won't undergo any reaction or change when it is mixed with kerosene.

By doing experiment in lab specific gravity of PPC cement is 2.79

4.1.5 Compressive strength (IS:4031-part 6-1988)

Compressive strength of cement is determined by a compressive strength test on mortar cubes compacted by means of a standard vibration machine. Standard sand (IS: 650) is used for the preparation of cement mortar. Compression testing machine (as per IS: 14858) was used for compression test on specimens as in Figure 4.5 i.e. cubes of dimensions 70.6mm×70.6mm×70.6mm [21].

Figure 4.5 - Casting of cubes

Compressive strength after   7 days curing – 17 MPa

Compressive strength after 21 days curing – 23 MPa

Compressive strength after 28 days curing – 35 MPa

4.1.6 Tensile strength (ASTM C307 - 03(2012))

Tensile Strength of Cement test was formerly used to have an indirect indication of compressive strength of cement. Briquettes are required for testing tensile strength of cement as in Figure 4.7. The moulds of briquettes are according to the ASTM standards Figure 4.8. A mould consists of three briquettes. These moulds are filled

Figure 4.6 - Tensile testing machine

with cement mortar mix with cement to sand ratio 1:3 [13].
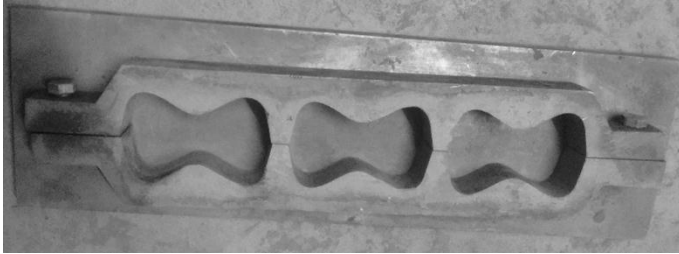
Figure 4.7 - Briquette mould
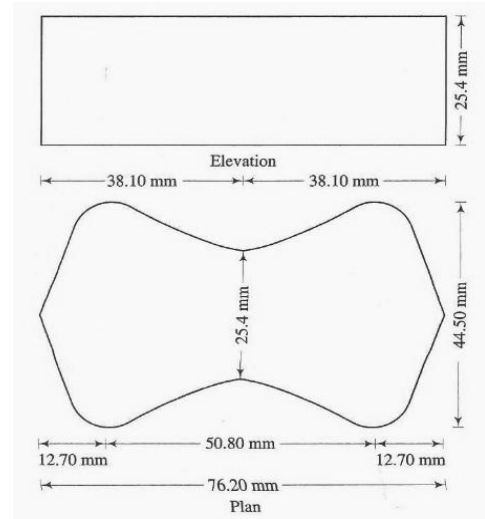
Figure 4.8 - Standard briquette

After 3 days and 7 days of curing, briquettes are tested in briquette testing machine Figure 4.6 to determine tensile Strength of cement mortar.

Tensile strength of cement after 3 days – 11 MPa.

Tensile strength of cement after 7 days – 16 MPa.

4.2 SAND

4.2.1 Specific gravity (IS-2720-PART-3-1980)

The specific gravity of sand was determined by both Pycnometer in Figure 4.9 and Density bottle in Figure 4.4. Sand particles composed of quartz have a specific gravity ranging from 2.65 to 2.67 [22].

Specific gravity of sand using density bottle = 2.576

Specific gravity of sand by using pycnometer = 2.837

Figure 4.9 - Pycnometer

Specific gravity obtained from density bottle is used for further calculations.

4.2.2 Grading of Fine Aggregates (IS:383 - 1970)

On the basis of particle size, fine aggregate is graded into four zones as per Table 4.1 [23].

Table 4.1 - Particle size distribution as per (IS: 383-1970)

IS Sieve	Percentage passing for			
	Grading Zone I	Grading Zone II	Grading Zone III	Grading Zone IV
10mm	100	100	100	100
4.75mm	90 – 100	90 – 100	90 – 100	95 – 100
2.36mm	60 – 95	75 – 100	85 – 100	95 – 100
1.18mm	30 – 70	55 – 90	75 – 100	90 – 100
0.60mm	15 – 34	35 – 59	60 – 79	80 – 100
0.30mm	5 – 20	8 – 30	12 – 40	15 – 50
0.15mm	0 - 10	0 – 10	0 - 10	0 – 15
Fineness Modulus	4.0 – 2.71	3.37 – 2.1	2.78 – 1.71	2.25 – 1.35

Sieve analysis of fine aggregates is done

Table 4.2 - Sieve analysis result

IS Sieve	Wt. retained (g)	Cum. Wt. retained (g)	Cum. percentage wt. Retained (%)	Weight passing (g)	Percentage passing (%)
10mm	0.00	0.00	0.00	986.10	100.00
4.75mm	6.00	6.00	0.61	980.10	99.39
2.36mm	8.50	14.50	1.47	971.60	98.53
1.18mm	9.50	24.00	2.43	962.10	97.57
0.60mm	12.70	36.70	3.72	949.40	96.28
0.30mm	80.10	116.80	11.84	869.30	88.16
0.15mm	775.30	892.10	90.47	94.00	9.53
Pan	94.00	986.10	**Total = 110.54**		
Total	986.10				

Note: Conforming to grading zone IV of Table 4.2 of IS: 383-1970

$$\text{Fineness modulus} = \frac{\text{cum.weight retained}}{100} = \frac{110.54}{100} = 1.10$$

After sieve analysis in Figure 4.10 it was found that the fine aggregates is conforming of zone IV standards and have a fineness modulus of 1.10

Fineness modulus of fine aggregate is 1.10. It means the average value of aggregate is in between the 0.15mm sieve and 0.30mm sieve. It means the average aggregate size is in between 0.15mm to 0.3mm.

Figure 4.10 - Sieve analysis

4.3   COARSE AGGREGATES

4.3.1   Water absorption (IS: 2386 - PART 3 - 1963)

Coarse aggregate have a tendency of absorbing water from the concrete mix. This reduction in water content, if not accounted for, can cause incomplete hydration of cement. The water absorption of aggregates ranges from 0.1 to 2.0 % [25]. This test is done as shown in Figure 4.11. Water absorption of aggregates = 1.413%

4.3.2   Specific gravity (IS: 2386 - PART 3 - 1963)

The specific gravity of aggregates can be calculated by the test results of water absorption test [25].

Figure 4.11 - Density basket

Effective specific gravity of aggregates = 2.68
Apparent specific gravity of aggregates = 2.745

4.4 ADDITIVE

4.4.1 Alccofine

Alccofine 1203 is slag based supplementary cementitious material (SCM) having ultra-fineness with optimized particle size distribution. Alccofine is a new generation, micro fine material of particle size much finer than other hydraulic materials like cement, fly ash, silica etc. as in Figure 4.12 being manufactured in India. Alccofine has unique characteristics to enhance 'performance of concrete' in fresh and hardened stages due to its optimized particle size distribution. It can be used as practical substitute for Silica Fume as it has optimum particle size distribution not too coarse, not too finer either. It lowers permeability of the mix. Resistance to chemical attack / corrosion is improved as ingression becomes difficult. Physical and chemical properties are shown in Table 4.3 and Table 4.4
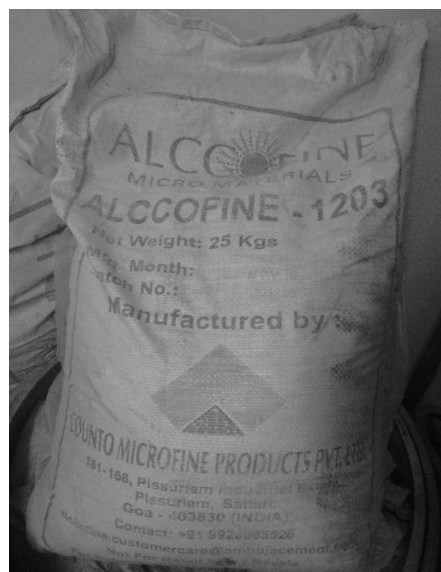
Figure 4.12 - Alccofine 1203

Table 4.3 - Physical parameters of Alccofine 1203 []

Specific gravity	Bulk Density (kg/m^3)	Particle size distribution (μ)		
		D 10	D 50	D 90
2.9	600-700	1 - 2	4 - 5	8 - 9

Table 4.4 - Chemical parameters of Alccofine 1203 []

CaO	Al$_2$O$_3$	SIO$_2$	Glass content
31-33%	23-25%	33-35%	>90%

4.4.2 Steel fibers

Crimped Steel Fibers - The steel fibers used were of crimped shape with length of 30mm and Diameter of 0.4mm as in Figure 4.13. The tensile strength of these fibers was 800-2500 MPa. Steel fibers have greater surface area then the reinforcement and hence, should corrode first. The rate of corrosion in reinforcement would be reduced due to shortage of fuel in the reaction, i.e. Water and oxygen.

Figure 4.13 - Crimped steel fibers

4.5 MIX DESIGN

The Concrete Mix Design has been done as per IS: 10262-2009

The characteristics compressive strength is 20 N/mm^2 i.e. M20 grade of concrete. Portland Pozzolana Cement has been used with specific gravity 2.79. The coarse aggregates used of maximum size 20mm angular, specific gravity of 2.68 and water absorption 1.413%. The fine aggregates had specific gravity of 2.576. Good degree of quality control has been maintained and only mild exposure was allowed. Concrete was designed for the workability of 0.90

TEST DATA FOR MATERIALS

a) Cement used – PPC
b) Specific gravity of cement = 2.79
c) Specific gravity of coarse aggregate = 2.68
d) Specific gravity of fine aggregate = 2.576
e) Water absorption of coarse aggregate = 1.413%

Water to cement ratio: 0.40

Table 4.5 - Mix design with water cement ratio 0.4

Water	Cement	Fine aggregate	Coarse aggregate
153.26 kg/m^3	383.16 kg/m^3	587.03 kg/m^3	1292.82 kg/m^3

Water to cement ratio: 0.45

Table 4.6 - Mix design with water cement ratio 0.45

Water	Cement	Fine aggregate	Coarse aggregate
153.26	340.59 kg/m^3	521.09 kg/m^3	1123.94 kg/m^3

Final Mix Design - 1 : 1.53 : 3.3

4.6 SPECIMENS

A sum total of 27 specimens have been casted as in Figure 4.15 and Figure 4.14. First 6 reference specimen were casted and checked for their corrosion and flexural strength. W/C ratio of 0.4 (A) and 0.45 (B) was taken. Effective cover depth of 50mm (X) and 45mm (Y) was used. Reinforcements of diameter 12mm (1), 16mm (2) and 20mm (3) were used in beams. The total length of reinforcement was 450mm i.e. 380mm within the beam and rest of 70mm exposed to atmosphere. Vibrating table was used for compaction of beams.

Figure 4.14 - Preparation of moulds

Figure 4.15 - Casting of specimens

The specimens were of the dimensions 400mm×100mm×100mm. In next 12 specimens, w/c ratio, cover depth and reinforcement diameter has been varied. Effective Cover depth of 50mm (X) and 45mm (Y) was provided. These were then tested for corrosion using Half-Cell Potential method. From the data the optimized W/C ratio and cover depth were obtained and then used further. Out of the rest of the 6 specimens, in 3 of them, 1% Steel fibers (S F) were added and in other 3, 1% steel fibers were added and 20% of the total cement was replaced by Alccofine (A F). The Optimized W/C ratio and cover depth were used.

Table 4.7 - Specimens for reference

S.No.	Specimens	Reinforcement diameter (mm)	Cover depth (mm)	w/c ratio
1.	A X 1	12	50	0.40
2.	A X 2	16	50	0.40
3.	A X 3	20	50	0.40
4.	B X 1	12	50	0.45
5.	B X 2	16	50	0.45
6.	B X 3	20	50	0.45

Table 4.8 – Specimens for corrosion

S.No.	Specimens	Reinforcement diameter (mm)	Cover depth (mm)	w/c ratio
1.	A X 1	12	50	0.40
2.	A Y 1	12	45	0.40
3.	A X 2	16	50	0.40
4.	A Y 2	16	45	0.40
5.	A X 3	20	50	0.40
6.	A Y 3	20	45	0.40
7.	B X 1	12	50	0.45
8.	B Y 1	12	45	0.45
9.	B X 2	16	50	0.45
10.	B Y 2	16	45	0.45
11.	B X 3	20	50	0.45
12.	B Y 3	20	45	0.45

Table 4.9 - Specimens for corrosion with additives

S.No.	Specimens	Reinforcement diameter (mm)	Cover depth (mm)	w/c ratio
1.	S F 1	12	50	0.40
2.	A F 1	12	50	0.40
3.	S F A F 1	12	50	0.40
4.	S F 2	16	50	0.40
5.	A F 2	16	50	0.40
6.	S F A F 2	16	50	0.40
7.	S F 3	20	50	0.40
8.	A F 3	20	50	0.40
9.	S F A F 3	20	50	0.40

The casted beams, after final setting, were fully submerged in clean water for 28 days of curing to achieve strength as shown in Figure 4.16.

Figure 4.16 - Curing of specimens

4.7   CORROSION TECHNIQUE

Impressed current experimental method is used to create corrosive environment for specimens as in Figure 4.17. The study done by Nabeel Shaikh and Sheetal Sahare [4] shows that for constant current density, higher voltage specimens show crack formation in shorter duration. After doing extrapolation from their data, it was determined that for 15V power supply the crack formation will occur within 5 days of accelerated curing.
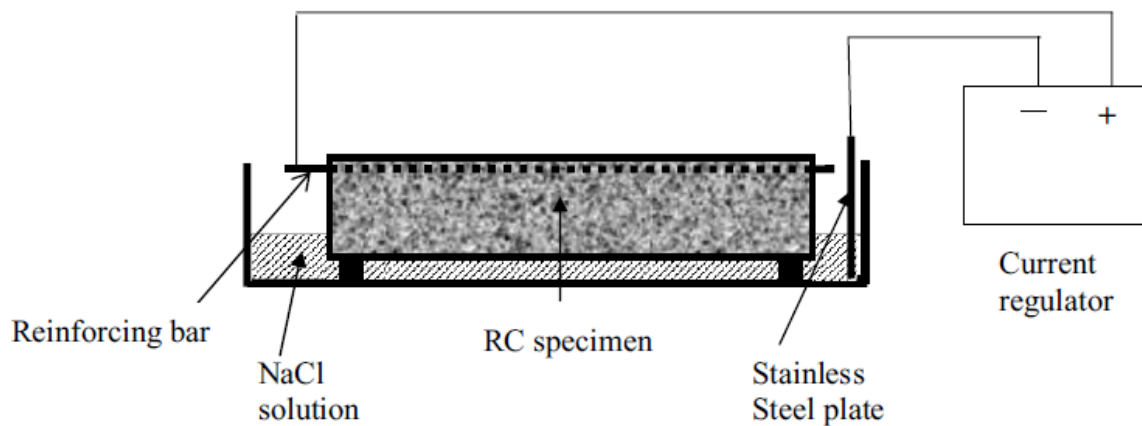
Figure 4.17 - Impressed current experimental method [4]

Accelerated corrosion technique - Specimens were placed in 3% NaCl solution Figure 4.18 with a constant voltage supply of 15V. Steel reinforcement was acting as anode and copper plate was the cathode as in Figure 4.19. This electrochemical cell was created in the lab to accelerate the rate of corrosion for the duration of 5 days.

Figure 4.19 - Setup for accelerated corrosion

Figure 4.18 - Specimen placed in 3% NaCl solution

After the completion of 5 days of accelerated corrosion technique the reinforcement would be corroded as in Figure 4.20 enough so that crack formation occurs as in Figure 4.22.
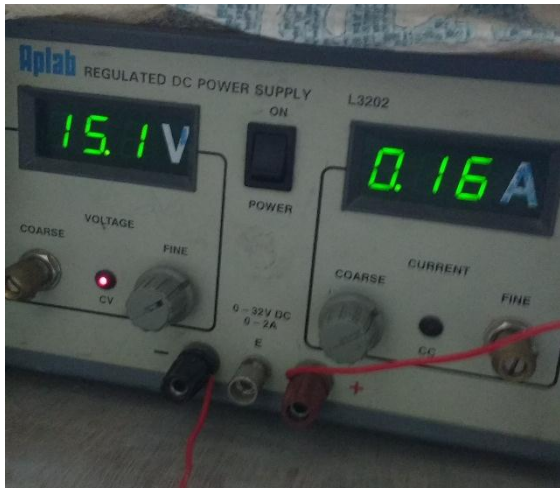
Figure 4.21 - Power supply (0-15V)

Figure 4.20 - Ongoing corrosion

Figure 4.22 - Cracking propagation due to corrosion

Figure 4.24 – Corrosion of steel fibers in SF specimen

Figure 4.23 - Corrosion of steel fibers in SF+A specimen

CHAPTER 5

RESULTS AND DISCUSSION

5.1 HALF-CELL POTENTIAL

The potential difference between the two half cells is related to the probability of corrosion. This potential difference or half-cell potential was measured using Cu/CuSo$_4$ half-cell with 1 M Copper sulphate solution. Setup is formed as shown in Figure 5.1. The relationship between half-cell potentials and corrosion probability is as per ASTM C876-91 in Table 3.1 [14].

Figure 5.1 - Half-cell potential setup

Table 5.1 - Half-cell potential of reference specimens

S.No.	Specimens	Half-Cell Potential (mV)	Corrosion probability
1.	A X 1	-173	10% no corrosion
2.	A X 2	-185	10% no corrosion
3.	A X 3	-192	10% no corrosion
4.	B X 1	-180	10% no corrosion
5.	B X 2	-207	Intermediate
6.	B X 3	-213	Intermediate

The half-cell potential values of reference specimens were greater than or close to -200mv which shows that there is very less probability of corrosion as shown in Table 5.1. With the increase in water to cement ratio, it is observed that the half-cell potential values are lowered.

The specimens with different water to cement ratio, cover depth and rebar diameter were tested by half-cell potential method and experimental data was collected.

Table 5.2 - Half-cell potential for corroded specimens

S.No.	Specimens	Half-Cell Potential (mV)	Corrosion probability
1.	A X 1	-387	90% corrosion
2.	A Y 1	-445	90% corrosion
3.	A X 2	-398	90% corrosion
4.	A Y 2	-464	90% corrosion
5.	A X 3	-494	90% corrosion
6.	A Y 3	-519	excessive corrosion
7.	B X 1	-598	excessive corrosion
8.	B Y 1	-605	excessive corrosion
9.	B X 2	-615	excessive corrosion
10.	B Y 2	-627	excessive corrosion
11.	B X 3	-604	excessive corrosion
12.	B Y 3	-633	excessive corrosion

The Experimental data shown in Table 5.2 represents the relationship between change in water to cement ratio, cover depth and reinforcement diameter on rate of corrosion. With the increase in water to cement ratio, it is observed that the half-cell potential values are lowered and corrosion rate increases. As the cover depth is increased, it is noticed that the half-cell potential values are slightly higher, hence rate of corrosion is decreased. With the increase in reinforcement diameter, the surface area of the rebar increases and also the required penetration depth decreases. Because of these factors the corrosion rate also increases.

The specimens with different combination of additives and rebar diameter were tested by half-cell potential method. The optimized water to cement ratio (0.4) and cover depth (50mm) were used in the specimens and experimental data was collected.

Table 5.3 - Half-cell potential for corroded specimens with additives

S.No.	Specimens	Half-Cell Potential (mV)	Corrosion probability
1.	S F 1	-505	excessive corrosion
2.	A F 1	-345	90% corrosion
3.	S F A F 1	-447	90% corrosion
4.	S F 2	-558	excessive corrosion
5.	A F 2	-362	90% corrosion
6.	S F A F 2	-483	90% corrosion
7.	S F 3	-581	excessive corrosion
8.	A F 3	-374	90% corrosion
9.	S F A F 3	-543	excessive corrosion

The Experimental data shown in Table 5.3 shows that the addition of steel fibers increases the half-cell potential values of the specimens because of the additional corrosion sites created by steel fibers acting as electrodes. Alccofine gives better packing efficiency to the concrete reducing the permeability of the mix. The lower half-cell potential values in case of Alccofine can be explained by this reduced portability. On the addition of both the additives the potential values comes out to be intermediate, with more pronounced effect of steel fibers. This is observed because the depth of steel fibers varies, with few of them being very close to the concrete surface hence more vulnerable to corrosion.

5.2 FLEXURAL STRENGTH

After the half-cell potential measurement's center point loading is done as shown in Figure 5.2 to determine the flexural strength of beams. Flexural strength is an important criteria for beams.

Figure 5.2 - Crack pattern at failure for flexure strength

Table 5.4 - Flexural strength of reference specimens

S.No.	Specimens	Reinforcement diameter (mm)	Cover depth (mm)	w/c ratio	Flexural strength (N\mm²)
1.	A X 1	12	50	0.40	21.51
2.	A X 2	16	50	0.40	24.62
3.	A X 3	20	50	0.40	29.88
4.	B X 1	12	50	0.45	21.20
5.	B X 2	16	50	0.45	23.85
6.	B X 3	20	50	0.45	29.26

As the experimental data shown in Table 5.4 and illustrated in Figure 5.3 it clearly shows that with the increase in water to cement ratio there is slight decrease in flexural strength of beams. As the reinforcement diameter increases the flexural strength also increases.
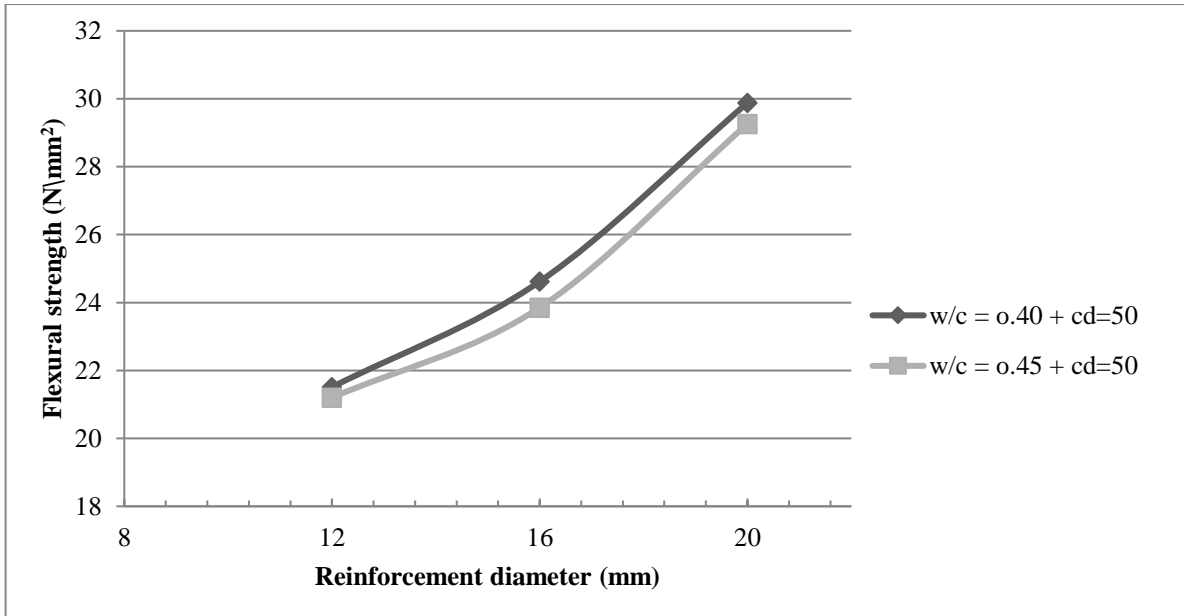
Figure 5.3 - Variation of Flexural strength w.r.t. rebar diameter

The specimens with different water to cement ratio, cover depth and rebar diameter were tested for their flexural strength and experimental data was collected.

Table 5.5 - Flexural strength of corroded specimens

S.No.	Specimens	Reinforcement diameter (mm)	Cover depth (mm)	w/c ratio	Flexural strength (N\mm²)
1.	A X 1	12	50	0.40	18.00
2.	A Y 1	12	45	0.40	17.01
3.	A X 2	16	50	0.40	19.44
4.	A Y 2	16	45	0.40	18.9
5.	A X 3	20	50	0.40	26.85
6.	A Y 3	20	45	0.40	25.65
7.	B X 1	12	50	0.45	17.60
8.	B Y 1	12	45	0.45	16.65
9.	B X 2	16	50	0.45	19.20
10.	B Y 2	16	45	0.45	18.40
11.	B X 3	20	50	0.45	26.55
12.	B Y 3	20	45	0.45	24.90

As the experimental data shown in Table 5.5 and illustrated in Figure 5.4 it clearly indicates that A Slight decrease in flexural strength is observed with increase in water to cement ratio. The cover depth, when increased provides resistance against corrosion, and hence preserves the flexural strength of beam after corrosion. The general trend is followed in case of change in reinforcement diameter, i.e. increase in flexural strength with increase in diameter.
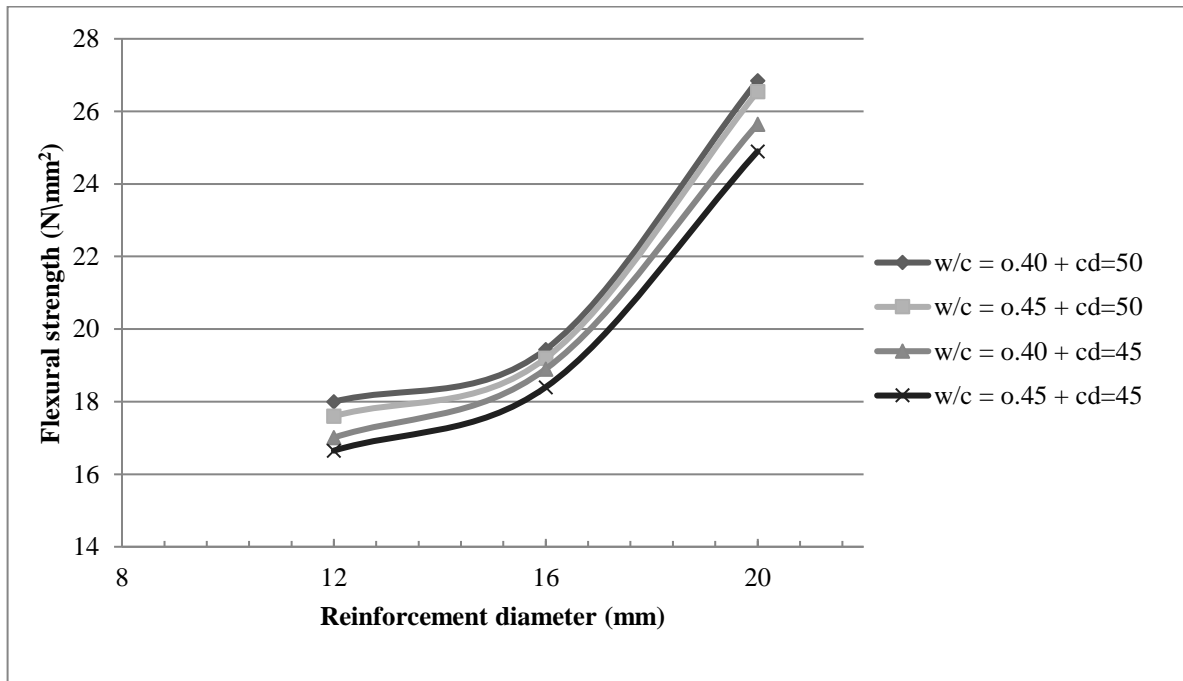
Figure 5.4 - Variation of Flexural strength w.r.t. rebar diameter of corroded beams

Table 5.6 - Percentage change in flexural strength

S.No.	Specimens	Flexural strength (N\mm^2)		Percentage change in Flexural strength (%)
		Without corrosion	With corrosion	
1.	A X 1	21.51	18	16.32
2.	A X 2	24.62	19.44	21.04
3.	A X 3	29.88	26.85	10.14
4.	B X 1	21.20	17.6	16.98
5.	B X 2	23.85	19.2	19.50
6.	B X 3	20	26.55	9.26

The specimens with different combination of additives and rebar diameter were tested for flexural strength. The optimized water to cement ratio (0.4) and cover depth (50mm) were used in the specimens and experimental data was collected.

Table 5.7 - Flexural strength of corroded specimens with additives

S.No.	Specimens	Reinforcement diameter (mm)	Cover depth (mm)	w/c ratio	Flexural strength (N\mm²)
1.	S F 1	12	50	0.40	21.02
2.	A F 1	12	50	0.40	21.38
3.	S F A F 1	12	50	0.40	21.87
4.	S F 2	16	50	0.40	24.66
5.	A F 2	16	50	0.40	25.29
6.	S F A F 2	16	50	0.40	25.79
7.	S F 3	20	50	0.40	29.03
8.	A F 3	20	50	0.40	29.57
9.	S F A F 3	20	50	0.40	30.60

As the experimental data shown in Table 5.7 and illustrated in Figure 5.5 it shows that Alccofine increases the density of the concrete specimen and reduces the corrosion, increasing the flexural strength of specimens. Corroded steel fibers increases the number of micro cracks because of the stresses generated by volume expansion these stresses are very low because of the low volume of the steel fibers. These micro cracks encourage the first crack formation. The further propagation of the crack is restricted by the steel fibers. The combination of both the additives has resulted in higher flexural strength of specimens from when they are individually used. The general trend is followed in case of change in reinforcement diameter, i.e. increase in flexural strength with increase in diameter.
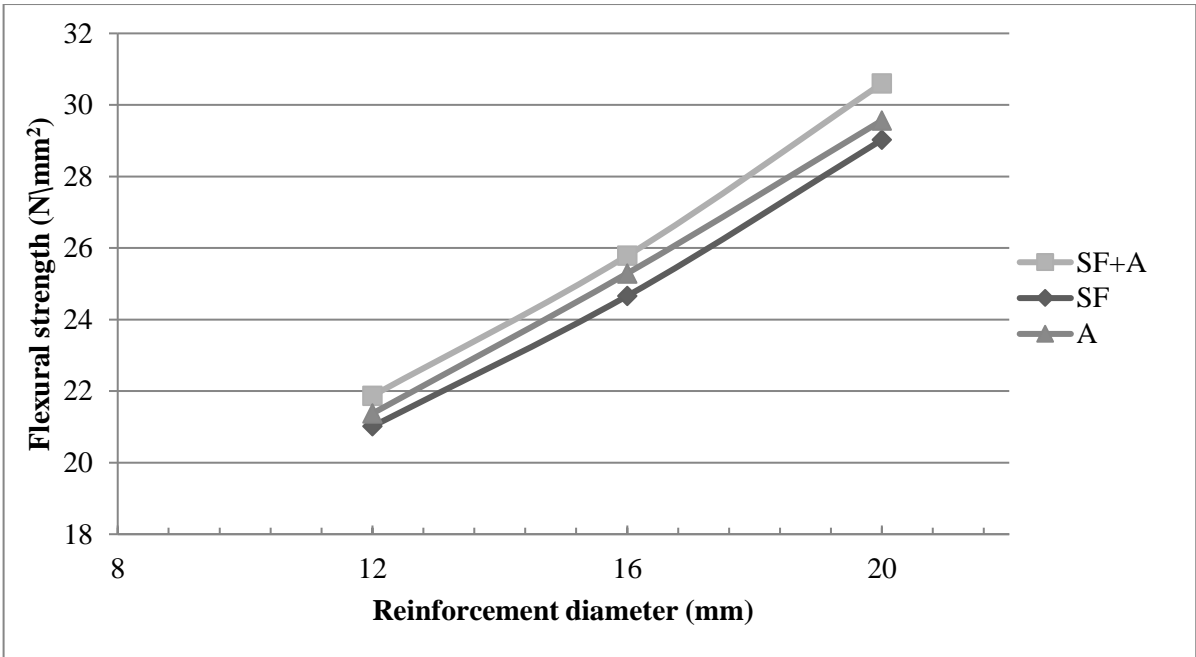
Figure 5.5 - Variation of Flexural strength w.r.t. rebar diameter of corroded beams with additives

CHAPTER 6

CONCLUSION

From all the experimental data collected until now, it can be concluded that:

- With the increase in water to cement ratio, it is observed that the half-cell potential values are lowered. Hence probability of corrosion increases.

- As the cover depth is increased, it is noticed that the half-cell potential values are slightly higher, hence rate of corrosion is decreased. With the increase in reinforcement diameter, the surface area of the rebar increases and also the required penetration depth decreases. Because of these factors the corrosion rate also increases.

- With the increase in water to cement ratio there is slight decrease in flexural strength of beams. As the reinforcement diameter increases the flexural strength also increases.

- The cover depth, when increased provides resistance against corrosion, and hence preserves the flexural strength of beam after corrosion. The general trend is followed in case of change in reinforcement diameter, i.e. increase in flexural strength with increase in diameter.

- On the addition of steel fibers, the half-cell potential values are increased because of the extra potential generated by the extra corrosion sites of steel fibers. The flexural strength remains unchanged.

- Alccofine, on the other hand reduced the half-cell potential values considerably, hence reducing the probability of corrosion. It also increases the flexural strength of the corroded reinforced beams.

- When used together, in case of half-cell potential values the effects seems to be subtractive, leaning more towards steel fibers but in case of flexural strength their effects become additive and increases the flexural strength considerably.

REFERENCES

1. Parvatareddy S. B. and Naidu G. G., (2017), "Comparative Study on Various Methods Used for Corrosion Protection of Rebar in Concrete", International Journal of Scientific Engineering and Technology Research, 6 (8), 1522-1527.

2. Altoubat, S., Maalej, M. and Shaikh, F. U. A., 2016, "Laboratory Simulation of Corrosion Damage in Reinforced concrete," International Journal of Concrete Structures and Materials, 10(3), pp.383-391.

3. K. Venkateswara Rao, B. Devi Pravallika and K. Phani Krishna, 2016, "An Experimental Study on Flexural Strength and Corrosion Properties of Reinforced Concrete Beams." International Journal of Engineering Research & Technology, 5(2), February-2016.

4. Nabeel Shaikh and Sheetal Sahare, (2016), "Effect of impressed current on corrosion of reinforcing bar in reinforced concrete", International Journal of Advances in Mechanical and Civil Engineering, 3 (1), 2016.

5. Kumar V., Singh R. and Quraishi M.A., (2013), "A study on corrosion of reinforcement in concrete and effect of inhibitor on service life of RCC", Journal of Materials and Environmental Sciences, 4 (5), 726-731.

6. ASTM C307-03(2012), Standard Test Method for Tensile Strength of Chemical-Resistant Mortar, Grouts, and Monolithic Surfacings, ASTM International, West Conshohocken, PA, 2012.

7. Poursaee, A., (2011), "Corrosion Measurement Techniques in Steel Reinforced Concrete" Journal of ASTM International, 8 (5), 1-15.

8. Dimitri V. Val, Leonid Chernin and Mark G. Stewart, (2009), "Experimental and Numerical Investigation of Corrosion-Induced Cover Cracking in Reinforced Concrete Structures" Journal of structural engineering, 2009, 135(4): 376-385.

9. Leelalerkiet V., Kyung J., Ohtsu M. and Yokota M., (2004), "Analysis of half-cell potential measurement for corrosion of reinforced concrete", Construction and Building Materials, 18, 155–162.

10. Ahmad S., (2003), "Reinforcement corrosion in concrete structures, its monitoring and service life prediction—A review", Cement and Concrete Composites 25, 459-471

11. BRE, John Broomfield Consultants, Risk Review Ltd, Trend 2000 Ltd & Indust. Adv., Report 2/DME 5.1, Handbook for corrosion rate measurements, 2001, 26p.

12. Technical Liaison Committee of the Institute of Corrosion and the Concrete Society, Half-cell potential surveys of reinforced concrete structures, Current Practice Sheet No. 120, Concrete, July/August 2000.

13. ASTM G1-90, 1999, "Standard Practice for Preparing, Cleaning, and Evaluating Corrosion Test Specimens," Annual Book of ASTM Standards, 3(2), ASTM International, West Conshohocken, PA, pp. 1–8.

14. ASTM C876-91, 1999 "Standard test method for half-cell potentials of un coated reinforcing steel in concrete"

15. IS: 5513, 1996, "Specification for Vicat's apparatus", Bureau of Indian Standards, New Delhi.

16. Silverman, D. C., 1990, "Simple Models/Practical Answers Using the Electrochemical Impedance Technique," Corrosion Testing and Evaluation, R. Baboian and W. Dean, Eds., ASTM International, West Conshohocken, PA.

17. Andrade, C., Marcias, A., 1990, Feliu, S., Escudero, M. L., and Gonzalez, J. A., "Quantitative Measurement of the Corrosion Rate Using a Small Counter Electrode in the Boundary of Passive and Corroded Zones of a Long Concrete Beam," Corrosion Rates of Steel in Concrete, ASTM STP 1065.

18. Newton, C. J. and Sykes, J. M., 1988, "A Galvanostatic Pulse Technique for Investigation of Steel Corrosion in Concrete," Corros. Sci., Vol. 2811, 1051–1074.

19. IS: 4031-part 4-1988, "Methods of physical tests for hydraulic cement", Indian Standards.

20. IS: 4031-part 5-1988, "Methods of physical tests for hydraulic cement", Indian Standards.

21. IS: 4031-part 6-1988, "Methods of physical tests for hydraulic cement", Indian Standards.

22. IS: 2720 (Part III/Sec I) - 1980," Methods of test for soils," Indian Standards.

23. IS: 383, 1970,"Specification for coarse and fine aggregates from natural sources for concrete", Indian Standards.

24. Andrade, C. and González, J. A., 1978, "Quantitative Measurements of Corrosion Rate of Reinforcing Steels Embedded in Concrete Using Polarization Resistance Measurements," Werkst. Korros. 29, 515–519.

25. IS: 2386 - PART 3 - 1963,"Methods of test for aggregates for concrete," Indian Standards.

26. Stern, M. and Geary, A. L., 1957, "Electrochemical Polarization: I. A Theoretical Analysis of the Shape of Polarization Curves," J. Electrochem. Soc., 104 (1), 56–63.